Synthesis and Properties of Polyamides and Polyesters On the basis of 2,2′-Bipyridine-5,5′-Dicarboxylic Acid and the Corresponding Polymer−Ruthenium Complexes

Sze Chit Yu, Sijian Hou, and Wai Kin Chan*

Department of Chemistry, University of Hong Kong, Pokfulam Road, Hong Kong

Received November 4, 1999; Revised Manuscript Received February 4, 2000

ABSTRACT: Two series of polyamides and polyesters derived from 2,2′-bipyridine-5,5′-dicarboxylic acid have been synthesized. Different types of aliphatic and aromatic diamine and diol monomers with different structure were polymerized with the diacid or diacid chloride by using different polymerization methods. Most of these polymers exhibited modest thermal stabilities with decomposition temperatures in the range 320−500 °C, depending on the structure of the polymer main chain. It was found that some polyamides with a rigid main chain formed a lyotropic mesophase when dissolved in concentrated sulfuric acid or HMPA−4% LiCl solvent systems. For those polyamides and polyesters with a more flexible main chain, a thermotropic liquid crystal phase was observed. If a long and flexible pendant chain was attached to the polyesters, side chain melting was observed before the onset of the crystalline−nematic transition. The 2,2′-bipyridyl moieties were able to form a complex with ruthenium. These polymer−ruthenium complexes were either synthesized by metalation of the polymers or synthesized directly from the corresponding ruthenium-containing monomer. After the formation of ruthenium complexes, they were able to enhance the photosensitivity and charge carrier mobility of the polymers. The ruthenium-containing polymers also emit red light at ca. 700 nm owing to the emission from the metal−ligand charge-transfer excited states. Some polymers with good film forming properties were fabricated into simple single-layer light-emitting devices, and red light emission was observed when the devices were subjected to forward bias.

Introduction

Research in the molecular ruthenium complexes of 2,2′-bipyridine $[Ru(bpy)_3]^{2+}$,[1] 2,2′:6′,2″-terpyridine $[Ru(tpy)_2]^{2+}$,[2] and other similar ligands has been a very interesting area because of their unique and specific photophysical and electrochemical properties. Different types of ruthenium-containing polymeric materials were reported in the literature. For example, polymers based on polystyrene,[3] polypyrroles,[4] π-conjugated poly(2,2′-bipyridine-5,5′diyl) and copolymers,[5] poly(vinylbipyridine),[6] polyesters,[7] poly(*p*-phenylenevinylene) with pendant terpyridine,[8] and electropolymerized bipyridine[9] or terpyridine[10] derivatives have been prepared. Some potential applications such as polymer-supported electrodes, photosensitizers, emission sensitizers, photogalvanic cells, and metal ion sensing have been proposed for these polymers.

Recently, there are several examples of using ruthenium-containing polymers for light-emitting and other optoelectronic applications.[11] The feasibility of incorporating the ruthenium complexes into the polymer main chain or side chain has been explored by our group. We have synthesized different kinds of rigid polymers containing polypyridine moieties. These polymers were functionalized with different bidentate[12] or tridentate[13] polypyridine ligands on the polymer main chain or side chain. The syntheses of some rigid rod aromatic polyamides and heterocyclic poly(benzobisazole)s derived from 2,2′-bipyridine-5,5′-dicarboxylic acid were also reported.[14] It was found that these polymers exhibited modest thermal stability and can form a lyotropic liquid crystal phase above the critical concentration. In addition, the bipyridine moiety in the polymer main chain is able to form a complex with different transition metals. The optical as well as the electronic properties can be manifested by the formation of metal complexes. It was found that the charge transport and other photonic properties were enhanced by the ruthenium complexes.[15] In addition, the photosensitivity was also extended to a longer wavelength due to the presence of the photosensitive ruthenium complexes.

Rigid rod polymers have attracted considerable interest because of their ability to form a liquid crystalline (LC) phase and their potential application as high modules and high performance thermoplastics.[16] For the high melting aromatic polyamides, liquid crystallinity is usually observed in solution of the polymers in specific solvents and can be referred to as a lyotropic behavior. Fiber spun from a lyotropic liquid crystal solution has a highly oriented, extended chain morphology, yielding a high strength and high modulus material. In contrast, the lower melting aromatic polyesters show thermotropic behavior because liquid crystallinity occurs in the melt within a specific temperature range. The structure of mesogenic units and polymer backbones and the nature of spacer connecting the mesogenic units with polymer backbones are the most important factors that influence the LC properties of the polymers. With respect to these considerations, we are interested in studying the relationships between the structure of the polymer backbone and its LC properties.

In this paper, we describe the comprehensive studies of two series of polyamides and polyesters by the polymerization of 2,2′-bipyridine-5,5′-dicarboxylic acid with various diamine and diol monomers. The syntheses of the polymers and their physical properties such as thermal stability and liquid crystalline properties were investigated. Moreover, we also studied the formation of polymer−ruthenium complexes and the effect of the metal to the optoelectronic properties such as photoconductivity, luminescence, and charge transport.

10.1021/ma991863j CCC: $19.00
Published on Web 04/06/2000

Scheme 1. Synthesis of Bipyridine-Based Polyamides

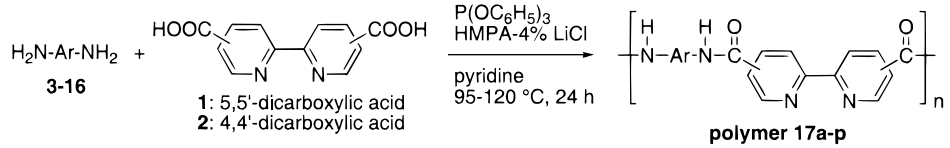

Diamines used for the synthesis of polyamides:

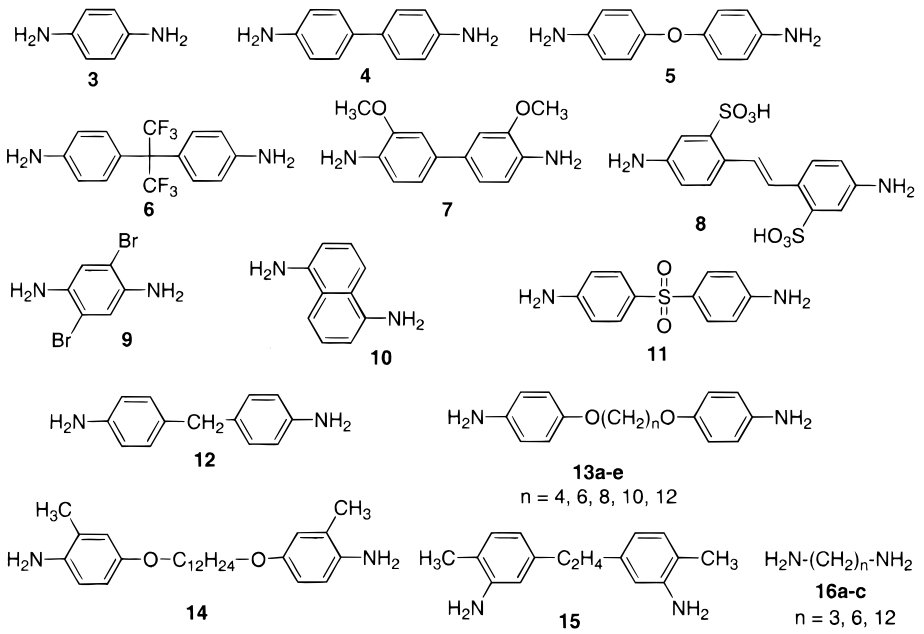

Results and Discussion

Synthesis of Polymers, Model Compounds and Their Corresponding Metal Complexes. Polyamides **17a**−**p** were synthesized in good yield by Yamazaki's method[17] using pyridine and triphenyl phosphite (TPP) as the condensing reagents (Scheme 1). Different aromatic (**3**−**15**) and aliphatic diamine monomers (**16a**−**c**) with different flexibility were used for the polymerization reactions. It was found that hexamethylphosphoramide (HMPA)−4% LiCl was the best solvent system for the polymerization reaction. Other polar aprotic solvents such as *N*,*N*-dimethylformamide (DMF), *N*-methyl-2-pyrrolidone (NMP), and *N*,*N*-dimethylacetamide (DMAc) were tried in the polymerization reaction. However, the oligomers precipitated from the reaction mixture even in the presence of LiCl or $CaCl_2$. The synthetic properties of these polymamides are summarized in Table 1. We also tried to synthesize polyamides based on 2,2′-bipyridine-4,4′-dicarboxylic acid **2**. Results showed that these polymers exhibited lower viscosity and decomposition temperature and they were not studied in detail.

For the polyesters, the most widely used reactions for the polymerization are transesterification or alcoholysis of acid chloride (Scheme 2). The former reaction was performed at high temperature in the melt, while the later one was carried out at medium/low temperatures in solution or by an interfacial reaction. Usually, transesterification proceeds smoothly with aliphatic diols bearing a primary or secondary hydroxyl group. It is generally not suitable for diols having aromatic or tertiary hydroxyl groups because of the poor nucleophilicity, competitive elimination reactions, and steric hindrance. In our studies, those polyesters derived from rigid aromatic diols (**22**−**29**) were synthesized by the reaction with 2,2′-bipyridine-5,5′-dicarbonyl chloride (**20**) in the presence of pyridine. Polyesters with a flexible main chain or side chain were synthesized by transesterification reaction between diethyl-2,2′-bipyridine-5,5′-dicarboxylate (**21**) and the corresponding diols (**30**−**38**) with a catalytic amount of titanium(IV) isopropoxide. This was found to be one of the most efficient catalysts for polymerization.[18,19] The yield of polymerization after purification was moderate to excellent (62−94%) depending on the type of monomers used (Table 2). The diethyl ester monomer **21** was used for polymerization because of its lower melting point and higher solubility in diols. Therefore, the reaction was easier to control, and the polymers obtained were of high quality. All the polyesters are soluble in 1,1,2,2-tetrachloroethane (TCE)/phenol mixture (1:1 w/w), and some of them are slightly soluble in NMP or DMF. Usually, polyesters with longer spacer linkages, with flexible side chains, or with substituted halogen atoms exhibit higher solubility in organic solvents.

To study the optimum condition for the polymer synthesis, metal complexation reaction, and structural characterization, we prepared different model complexes (**18**−**19**, **40**, Scheme 3). They were prepared by the same procedures as the polymerization reaction in good yield, and their spectroscopic properties were studied.

The syntheses of the polyamide− or polyester−ruthenium complexes are shown in Scheme 4. In general, there are two methods to incorporate the ruthenium to the 2,2′-bipyridine moiety on the polymer main chain. The first method (method A) involves the polymerization of the ruthenium-containing monomers (**Ru-1** or **Ru-2**) with another monomer. By using this method, the metal content in the polymer is relatively easier to control. However, the chemical and thermal

Table 1. Synthesis and Properties of Polyamides Based on Diacid Monomer 1

polyamide	diamine monomer	reaction temp (°C)	yield (%)[a]	η_{inh} (dL/g)[b]	T_d (°C)[c]	thermal transition process(es)[d]	lyotropic liquid crystal[e]	thermotropic liquid crystal[e]
17a	**3**	120	92	0.25	410	T_g − 364 °C	+	−
17b	**4**	120	93	1.11	498	T_g − 404 °C	+	−
17c	**5**	120	93	0.51	464	T_g − 316 °C	+	−
17d	**6**	90	85	0.46	415	T_g − 220 °C	−	−
17e	**7**	120	94	0.79	350	T_g − 203 °C	+	−
17f	**8**	120	75	0.64	375		−	−
17g	**9**	120	72	0.38	319	T_g − 239 °C	−	−
17h	**10**	120	96	0.53	412		+	−
17i	**11**	120	79	0.65	433		−	−
17j	**12**	90	88	0.44	390		+	−
17k1	**13a**	90	90	0.12	380	T_g − 223 °C	−	−
17k2	**13b**	90	94	0.12	380	T_g − 216 °C	−	−
17k3	**13c**	90	92	0.36	376	K→N 322 °C N→I 338 °C	−	+
17k4	**13d**	90	95	0.41	372	K→N 299 °C N→I 338 °C	−	+
17k5	**13e**	90	93	0.48	371	K→N 272 °C N→I 350 °C	−	+
17m	**14**	90	91	0.61	410	K→N 298 °C N→I 366 °C	−	+
17n	**15**	120	83	0.52	392	T_g − 209 °C	−	−
17p1	**16a**	90	73	0.28	371	T_g − 154 °C	−	−
17p2	**16b**	90	82	0.21	360	T_g−163 °C	−	−
17p3	**16c**	90	76	0.35	362	T_g−132 °C K→N 307 °C N→I 332 °C	−	+

[a] Yield after purification. [b] Inherent viscosity measured in 98% H_2SO_4 at 30 °C with $c = 0.5$ g/dL. [c] Decomposition temperature determined by TGA under N_2 atmosphere. [d] T_g: glass transition temperature. K: crystalline (solid) phase. N: nematic phase. I: isotropic phase. [e] Key: (+) observed; (−) not observed.

stabilities of the metal complex may limit its use when a rigorous polymerization condition is required. In the second method (method B), the metal complexation reaction is carried out between the metal-free polymer and the ruthenium complexes. A less rigorous condition is normally used, but the metal loading is usually lower and it lacks the certainty to the amount of metal incorporated in the polymer. In our studies, the metal complexation of the polyamides can be achieved by both methods. By treating the polyamides **17b** with the activated ruthenium complex $Ru(bpy)_2(OTf)_2(acetone)_2$, the polyamide−ruthenium complex **Ru-17b** was obtained**.**

Method A was employed to prepare the polyamide ruthenium complexes because complexes **Ru-1**,**2** were able to survive in the polymerization condition. Model complexes **18**−**19** were synthesized by the reaction between **Ru-1** or **Ru-2** and toluidine in a mixture of triphenyl phosphite, pyridine, and HMPA−4%LiCl. ^{1}H NMR and FABMS studies showed that there was no ligand exchange in these reactions. A series of polyamides with different ruthenium loading (**Ru-17b1** to **Ru-17-b5**, **Ru-17d,f,h**) were prepared via method A and some of their physical properties are summarized in Table 3. The ruthenium contents of the polymers obtained from this method were in general higher than those obtained from method B. For the polyesters, their ruthenium complexes were synthesized via method B because **Ru-1** could neither melt nor survive in refluxing thionyl chloride. Model complex **40** was obtained in good yield by the reaction between ligand **39** and $Ru(bpy)_2(OTf)_2(acetone)_2$.

To confirm the ruthenium content in the polymers, the polymer−ruthenium complexes were digested with concentrated nitric acid and the ruthenium content of the resulting solution was determined by inductively coupled plasma spectroscopy (ICP). It was found that those ruthenium-containing polymers synthesized from method B had the ruthenium content of approximately 40−50% of the theoretical values (based on complete metalation), while those synthesized from method A had higher ruthenium content (∼70−80%) The inconsistency between the metal contents is probably due to the bulkiness of the $[Ru(bpy)_3]^{2+}$ species which lower the reactivity of the monomer.

Structure Characterization. Polyamides **17a**−**c**, **17e**, and **17g**−**p** are insoluble in common organic solvents but are soluble in polar aprotic solvents with alkaline metal salts such as NMP and HMPA with 4% LiCl. They are also soluble in organic acids such as trifluoroacetic acid and formic acid. Polyamide **17d** contains hexafluoroisopropylidene groups on the main chain and is soluble in solvents such as DMF, DMSO, and DMAc. Polyamide **17f** consists of with two sulfonic acid groups and is soluble in water. All the polyamide ruthenium complexes are soluble in polar aprotic solvents except **Ru-17b1** owing to its lower metal content. The ^{1}H NMR spectrum of polyamide **17d** in DMSO-d_6 is shown in Figure 1. The signals for the 2,2′-bipyridyl protons appear at ca. 9.6, 9.1, and 8.7 ppm, while the resonance signal due to the diamine monomer appears at 7.5−7.7 ppm.

The UV−vis spectra of the polymers are in general characterized by the absorption peaks due to the bipyridine intraligand $\pi-\pi^*$ transition at ca. 290−310 nm. After the formation of the polymer−ruthenium complex, an additional intense absorption band due to the metal−ligand charge transfer (MLCT) d−π^* transition can be found at ca. 500 nm, depending on the nature of the ligand. The UV−vis absorption spectra of polyamide **17b** and its corresponding complexes **Ru-17b1**−**5** are shown in Figure 2. The metal-free polyamide exhibits an intense absorption peak at 284 and 322 nm attributed to the absorption by the bipyridine ligand and the main

Scheme 2. Synthesis of Bipyridine-Based Polyesters by Using Alcoholysis of 2,2′-Bipyridine-5,5′-dicarbonyl Chloride or by a Transesterification Reaction

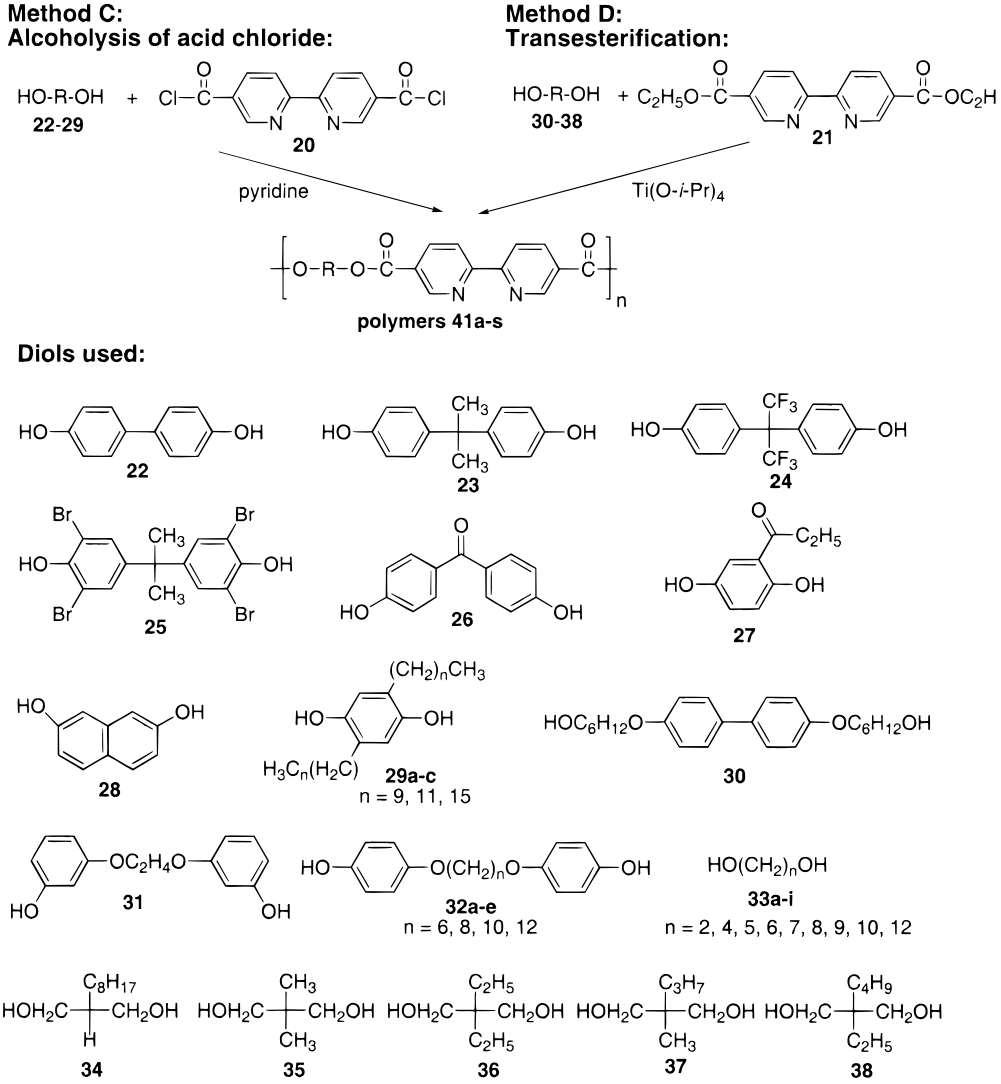

chain biphenyl unit, respectively. After the formation of the polymer−ruthenium complexes, the absorption due to the biphenyl unit shifted to 304 nm. The shift is a result of the distortion of the biphenyl ring due to the presence of the bulky $[Ru(bpy)_3]^{2+}$ moieties. The MLCT transition band, which is a characteristic absorption for ruthenium bipyridyl complexes, was found at 504 nm.

Figure 3 shows the absorption spectra of polyester **41k4** and its ruthenium complex. This polymer shows a broad and featureless absorption with only one intraligand transition peak at 302 nm. **Ru-41k4** shows an absorption peak at 293 nm which is slightly blue-shifted compared to the metal-free polymer. The MLCT transition is observed at 456 nm. All the polyesters and their ruthenium complexes exhibit very similar absorption features which are characterized by the ligand center transitions as well as the MLCT transitions.

In the FTIR spectra, the polyamides show characteristic absorption bands due to the amide C═O stretching and pyridine C═N stretching at 1640 and 1600 cm^{-1}, respectively. For the polyesters, the ester C═O stretching band is found near 1740 cm^{-1} while the pyridine ring C═N stretching band appear at the same position as the polyamides. After the formation of polymer metal complex, a very strong band is found at 840 cm^{-1} due to the P−F stretching of the counteranions.

Molecular Weight Measurements. Since the polyamides are only soluble in acids, we were not able to determine the molecular weight by gel permeation chromatography. The molecular weight of some polyamides were studied by using static light scattering technique from which the absolute weight-average molecular weight can be obtained. The relationship between the light scattering from a dilute polymer solution and the weight-average molecular weight can be described by the Zimm formalism

$$\frac{Kc}{R(\theta)} = \frac{1}{P(\theta)M_w} + 2A_2c$$

where K is the optical constant, $(2\pi^2(n\ dn/dc)^2/\lambda_0{}^4N_A)$, n is the refractive index of the solvent, dn/dc is the refractive index increment with respect to concentration, λ_0 is the wavelength in a vacuum, N_A is Avogadro's constant, c is the concentration (in g/mL), $R(\theta)$ is the Rayleigh ration at the angle of measurement, $P(\theta)$ is the particle scattering function, M_w is the weight-average molecular weight, and A_2 is the second virial coefficient. This equation can be solved graphically with a Zimm plot, in which $Kc/R(\theta)$ is plotted as a function of $\sin^2(\theta/2) + kc$, where k is a scaling factor. By extrapolation to zero concentration as well as zero angle,

Table 2. Synthesis and Properties of Polyesters Based on 2,2′-Bipyridine

polymer	diol	method[a]	yield (%)[b]	η_{inh} (dL/g)[c]	T_d (°C)[d]	T_g (°C)[e]	T_m (°C)[f]	T_i (°C)[g]	thermotropic liquid crystal
41a	**22**	I	76	0.76	442	324			−
41b	**23**	I	74	0.51	407	297			−
41c	**24**	I	60	0.41	418	291	391		−
41d	**25**	I	62	0.44	397	312	392		−
41e	**26**	I	73	0.37	427	286			−
41f	**27**	I	75	0.55	418	310			−
41g	**28**	I	77	0.53	404	284			−
41h1	**29a**	I	82	0.51	320	91	113	*j*	+
41h2	**29b**	I	83	0.58	332	101	115	*j*	+
41h3	**29c**	I	86	0.53	340	108	116	*j*	+
41i	**30**	II	86	0.68	397	214	236[h]	*i*	+
41j	**31**	II	86	0.59	409	190	280		−
41k1	**32a**	II	89	0.62	405	231	309	*j*	+
41k2	**32b**	II	94	0.59	400	215	294	*j*	+
41k3	**32c**	II	87	0.53	411	185	271	*j*	+
41k4	**32d**	II	90	0.58	416	156	269	*j*	+
41m1	**33a**	II	71	0.11	354		267		−
41m2	**33b**	II	82	0.34	378	270	285	319	+
41m3	**33c**	II	84	0.41	350	185	207[h]	*i*	+
41m4	**33d**	II	86	0.40	377	240	281[h]	*i*	+
41m5	**33e**	II	86	0.38	347	172	202[h]	*i*	+
41m6	**33f**	II	90	0.40	377	228	244	249	+
41m7	**33 g**	II	84	0.37	360	150	196	207	+
41m8	**33h**	II	86	0.40	372	182	213	220	+
41m9	**33i**	II	87	0.43	372	154	184	195	+
41n	**34**	II	84	0.39	371		172	190	+
41p	**35**	II	85	0.37	362		191	213	+
41q	**36**	II	90	0.49	368	125	201	286	+
41r	**37**	II	83	0.34	372		131	151	+
41s	**38**	II	87	0.33	382		138	155	+

[a] Method I: alcoholysis of acid chloride **20**. Method II: transesterification using monomer **21** as the starting material. [b] Yield after purification. [c] Inherent viscosity measured in 1,1,2,2-tetrachloroethane/phenol (1:1 w/w) at 30 °C with $c = 0.5$ g/dL. [d] Decomposition temperature determined by TGA under N_2 atmosphere. [e] Glass transition temperature. [f] Transition temperature from solid to liquid (or liquid crystal) phase. [g] Transition temperature from liquid crystal to isotropic phase. [h] A broad endothermic peak was observed. [i] The melting and isotropization temperature were very close, and they appeared as one single broad peak. [j] The polymer decomposed before isotropization temperature.

the M_w and A_2 values of the corresponding polymer can be obtained. Some polyamides with very high solubility in formic acid were chosen for studies. Figure 4 shows a typical Zimm plot for polyamide **17h** dissolved in 98% formic acid. The weight-average molecular weight M_w of the polyamides under studied are in the range between 20 000 and 40 000. It can be seen that the A_2 values of these polymers are on the order of 10^{-2} mol mL/g^2 (Table 4), which indicates a very strong polymer−solvent interaction. This is in accordance with the fact that solvation of polyamide requires the protonation of polymer molecules by the acid. After the formation of ruthenium complexes, polyamide **17j** showed a dramatic increase in molecular weight owing to the presence of the bulky ruthenium complexes.

Thermal Properties. The thermal properties of polyamides and polyesters are summarized in Tables 1 and 2. In general, the glass transition and decomposition temperatures of the polymers increase with the rigidity of the polymer main chain. For polymers with similar rigidity, both polyamides and polyesters exhibit similar decomposition temperature. It can be observed that polyamides **17b** and **17c** exhibit the highest T_g among all the polymers due to the rigid phenylene or biphenyl moieties in the main chain. Intermolecular hydrogen bonding might also enhance their thermal stabilities. For the polyesters, high T_g values are observed in aromatic polyesters **41a**−**g** presumably due to the rigid 2,2′-bipyridyl and the para-substituted phenylene units. These units significantly increase the chain rigidity of the respective polyester which results in decrease in free volume, high glass transition temperature, and absence of melting temperature in some of these polymers. On the other hand, those polymers derived from aliphatic diamines (polyamides **17p1**−**17p3**) or aliphatic diols (polyesters **41m1**−**41m9**) and those with pendant groups (polyamides **17g**,**m**; polyesters **41f**, **41h1**−**41h3**, and **41n**−**s**) or a flexible main chain (polyamides **17k1**−**17k5 17m**; polyesters **41i**, **41k1**−**41k4**) have a lower glass transition or decomposition temperature.

After the formation of metal complexes, the thermal stability of the polymers decreased. The decomposition temperatures of the polymer metal complexes are quite similar to the model compounds. The presence of the bulky ruthenium bipyridine complexes may distort the packing of polymer molecules. In addition, the ruthenium complex may decompose first and is subject to weight loss when it is being heated.

Thermotropic Liquid Crystal Properties. The liquid crystal properties of the polymers were evaluated by polarized optical microscopy. One characteristic of aromatic polyamides is their high melting point due to the hydrogen bonding and strong intermolecular attraction. The rigid polyamides decompose before reaching the mesomorphic phase. It was found that only those polyamides with a long and flexible main chain (**17k3**−**17k5 17m**, and **17p3**) exhibited thermotropic mesophase transition. Their transition temperatures are shown in Table 1. When viewed under a polarized microscope, these polymers show typical Schlieren texture for the nematic mesophase. Jahnig[20] and Ohtsuki[21] et al. suggested that the formation of the

Scheme 3. Synthesis of Model Metal Complexes

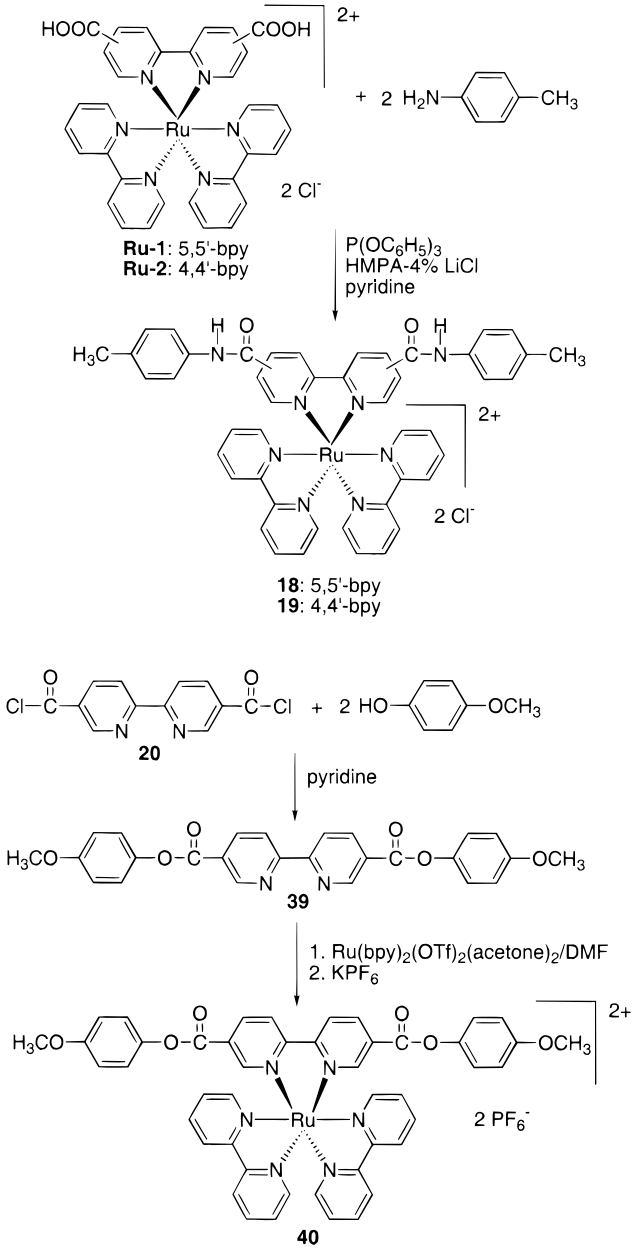

nematic phase in flexible rodlike polymers originated from the intra- and intermolecular interaction, and the structure−property relationships of some aromatic polyesters were studied. The conformation of the polymer backbone should affect the mesophase formation in main chain polymers consisting of nonconventional and flexible rodlike segment. Here, the thermotropic mesomorphic behaviors of four types of polyester are described: type I polyesters contain rigid or semirigid rodlike segments (**41a**−**g**); type II aromatic polyesters contain long alkyl pendent groups (**41h1**−**h3**); type III polyesters contain long and flexible main chain (**41k1**−**k4, 41m1**−**m9**); and type IV aliphatic polyesters contain branched spacers (**41n**−**s**). Type I polyesters do not exhibit any thermotropic LC behavior owing to the molecular rigidities. Most of the type II, II, and IV polyesters melted with strong birefringence and they showed nematic threaded-Schlieren textures in the liquid state. The phase transition behaviors of the polyesters are summarized in Table 2. Figure 5a shows the polarized micrograph for polyester **41m8** in which point singularities with $S = {}^1/_2$ and 1 were observed, which is the characteristic features for the nematic LC phase.

For the type II polyesters, they are able to form a layer structure in the liquid crystal state when the alkyl side chains reach a critical length.[22,23] Figure 6 shows the DSC thermogram of polymer **41h2**. The sample was first heated to the isotropic phase and then cooled slowly to room temperature. Two thermal transitions were observed at 101 and 113 °C. The first endothermic process was assigned to the side chain melting. Polarized microscope results indicated that the endothermic transition at 113 °C is the transition from solid to nematic phase. In these layer structures, the formation of mesophase is the result of lack of positional order with respect to the main chain packing within a layer. Owing to the melted side chains, a disordered sheath is formed around the backbone that screens the polymer chains from their neighbors. Therefore, the intermolecular positional orders, both parallel and perpendicular to the chain direction, are lost.[24] As a result, polymers **41h1**−**h3** exhibit the lowest melting points among the polyesters being studied.

The introduction of a spacer to the main chain can effectively reduce the melting transition temperature while the liquid crystal properties are retained. The melting temperatures of type III polyesters **41k1**−**k4** increased from 269 to 309 °C when the number of methylene units was decreased from 12 to 6. No isotropic transition was observed before decomposition. Figure 7 demonstrates the DSC traces of polymer **41k2**. The pristine polymer exhibited multiple thermal transitions on the first DSC scan. After the polymer was annealed at 280 °C for 24 h, two endothermic transitions were observed at 209 and 295 °C. The first transition may correspond to a transition in the solid phase while the second one is the crystal-mesophase transition. The melting temperature did not change noticeably between the first and second scans but the T_g shifted from 225 to 209 °C. Polyesters **41m2**−**m9** exhibit similar trend in thermal properties. When the number of methylene units n in the main chain was increased, the transition temperature decreased. Nematic mesophase were also observed in these polymers. A plot of melting temperature vs number of methylene units in the spacer is presented in Figure 8. This plot shows a typical odd−even number effect. Polymers with a even number of methylene spacers showed higher melting temperatures than those with odd numbered ones. This odd−even alternation was more pronounced for the lower homologues, and the effect diminished as n was increased. Similar odd−even oscillations were observed in other main chain LC polymers.[25,26] It is also interesting to note that polyesters **41m3**−**m5** only exhibit a very broad nematic−isotropic endothermic peak in the DSC thermograms. We suggest that both the LC and isotropic phases coexist at this temperature, which leads to a broad peak. However, if the samples were properly annealed just below the isotropic temperature for 24 h, the board peaks could be barely resolved into two separate peaks.

For the type IV polyesters, the melting T_m and isotropic temperatures T_i for polymer **41n** with a pendant octyl group were found to be 172 and 190 °C, respectively. These values are much higher than those polymers with asymmetrically disubstituted propylene units (**41r**, $T_m = 155$, $T_i = 151$ °C; **41s**, $T_m = 138$, $T_i =$

Scheme 4. Incorporation of Ruthenium Complexes into the Polymers

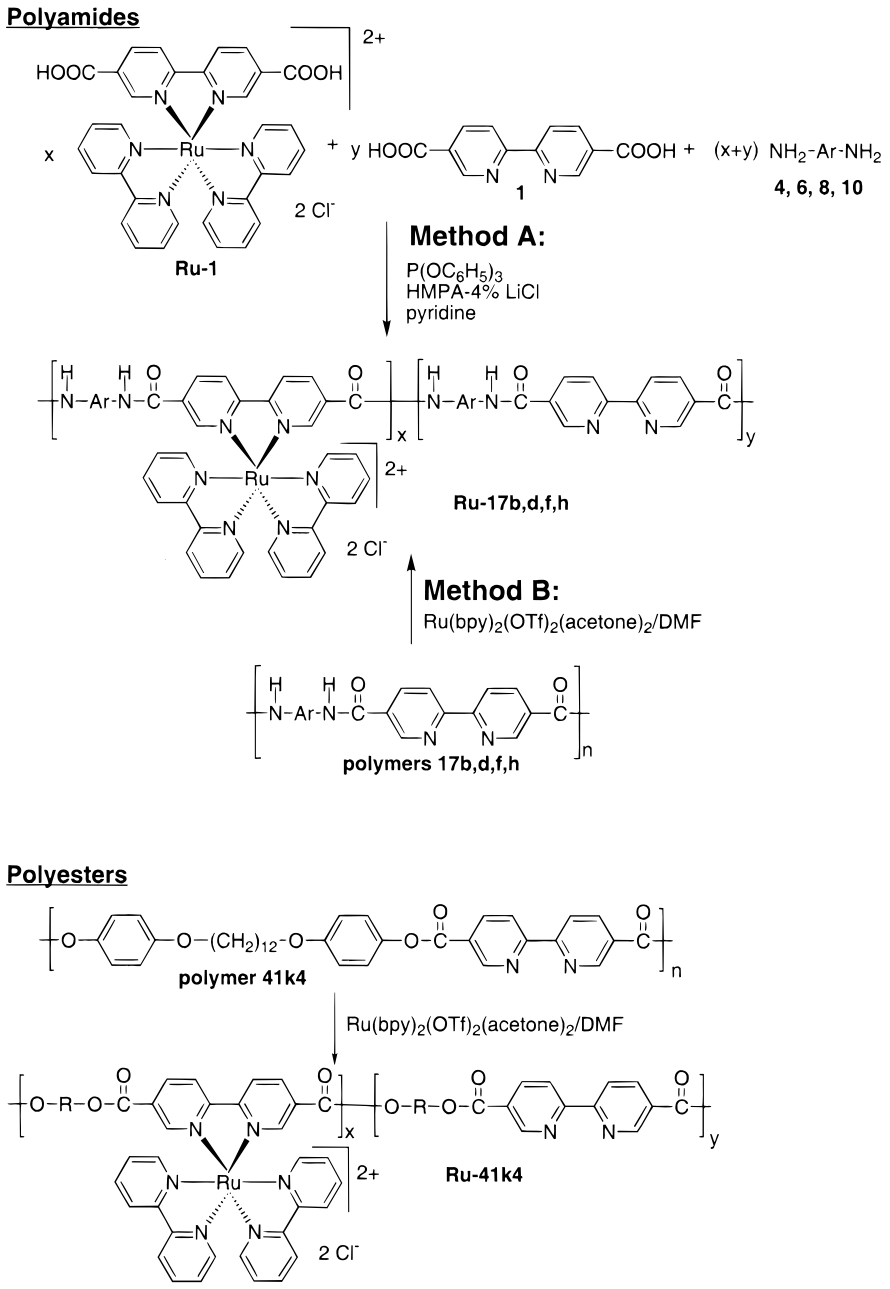

131 °C). Typical polarized micrograph for polymer **41n** is shown in Figure 5b. A typical threaded texture of nematic phase was observed when the polymer was heated near 190 °C. For polymers with symmetrically substituted alkyl pendant groups (**41p**,**q**), they exhibited higher melting temperature (T_m = 191, 201 °C) compared to those of the asymmetric ones. Obviously, by comparing the thermal transition temperatures between the type III and type IV polyesters, the asymmetric pendant groups can decrease the transition temperature to a greater extent than the main chain flexible spacers.

Lyotropic Liquid Crystal Properties. The rigid polyamides did not show any thermotropic LC properties. Instead, when these polyamides were dissolved in suitable solvents, lyotropic mesophases were observed above the critical concentration. The formation of lyotropic mesophase was confirmed by polarized microscopy under which a stir opalescence or birefringence was observed. A series of polyamide solutions in HMPA−4% LiCl or in 98% H_2SO_4 with different concentration was prepared. It was found that only polyamides **17a**−**c**,**h**,**j** exhibited lyotropic mesophases in both solvent systems. However, the lyotropic mesophases in H_2SO_4 formed very slowly, and it took more than 4 days to show an anisotropic pattern under polarized microscope. Therefore, detailed studies on the polymer solution were carried out in HMPA−4% LiCl. The critical concentrations for the formation of lyotropic mesophase were quite low. Polyamide **17b** formed a lyotropic mesophase at a concentration as low as 1%, which is significantly lower than the critical concentration of some well-studied aromatic polyamides.[27] On the other hand, when the concentration of polymer solution was increased further, mixtures of viscous polymer gel and lyotropic liquid crystal phase were obtained. As a result, the determination of clearing temperature became more difficult. A plot of the clearing temperature vs solution concentration (% w/w) for different polyamide and ruthenium complexes is shown in Figure 9. Polyamides with rigid main chain (**17a**,**b**,**h**) have higher clearing

Table 3. Synthesis and Properties of the Ruthenium-Containing Polyamides Prepared from Ru-1 and Different Diamine Monomers via Method A

polymer−ruthenium complex	diamine	x^a	y^a	yield (%)[b]	T_d (°C)[c]	λ_{max}/nm (a/L g^{-1} cm^{-1})[d]
Ru-17b1	**4**	0.2	0.8	92	351	256 (23)
						288 (48)
						318 (64)
						504 (3.2)
Ru-17b2	**4**	0.35	0.65	89	355	258 (27)
						288 (54)
						312 (56)
						504 (3.2)
Ru-17b3	**4**	0.5	0.5	73	338	258 (27)
						288 (70)
						306 (65)
						504 (4.0)
Ru-17b4	**4**	0.75	0.25	62	321	260 (24)
						288 (92)
						304 (67)
						504 (5.3)
Ru-17b5	**4**	1	0	60	320	262 (35)
						288 (94)
						304 (68)
						504 (6.5)
Ru-17d	**6**	0.5	0.5	83	331	260 (45)
						286 (67)
						312 (59)
						504 (4.6)
Ru-17f	**8**	0.5	0.5	68	327	258 (45)
						288 (70)
						502 (5.7)
Ru-17h	**10**	0.5	0.5	82	320	260 (58)
						286 (75)
						312 (76)
						516 (4.9)

[a] Feeding ratio of two monomers. [b] Yield after purification. [c] Decomposition temperature determined by TGA under N_2 atmosphere. [d] Absorption coefficient at the peak maxima.

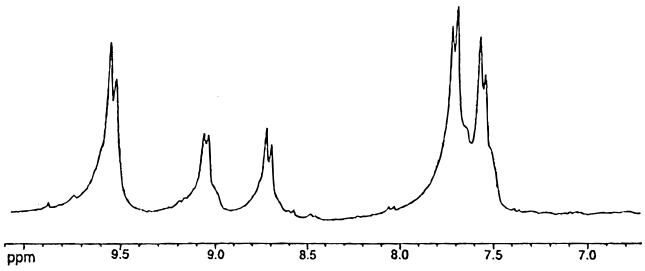

Figure 1. ^{1}H NMR spectrum of polyamide **17d** in DMSO-d_6.

temperature than those with more flexible main chain (**17c**) or pendant group (**17e**) because the efficient packing between polymer molecules may increase their stabilities in the solvent. Polyamide **17j** has a structure analogous to **17c**, and they both exhibited similar clearing temperatures due to their bent molecular structure. These observations suggest that the stability of the lyotropic mesophase strongly depends on the flexibility of the polymer backbone.

The lyotropic LC behavior of some polyamide ruthenium complexes were also studied. It was found only those polymers with low metal loading (**Ru-17b1**,**b2**) exhibited lyotropic mesophases, and the clearing temperature decreased from 82 to 71 °C (c = 4.3 wt %) when the ruthenium content was increased from 20 to 35% (Figure 9). The critical concentration also increased from 2.5 to 3.5 wt %. It is because the alignment of polymer molecules in the anisotropic phase is destroyed by the introduction of very bulky metal complexes. A polarized micrograph for the polyamide ruthenium complex **Ru-17b2** is shown in Figure 5c. When the ruthenium content was further increased to 50%, no lyotropic mesophase was observed.

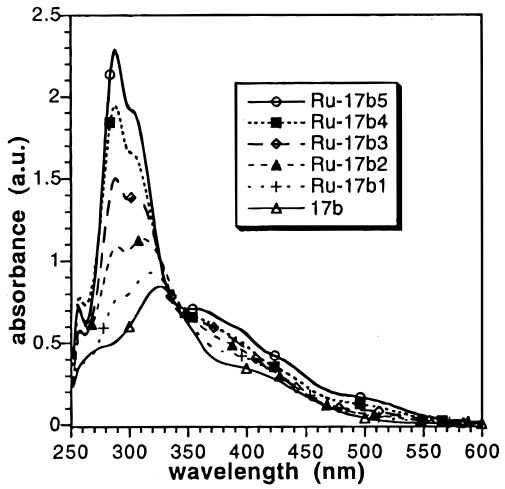

Figure 2. UV−vis absorption spectra of polyamide **17b** and its corresponding complexes in formic acid with different ruthenium loadings.

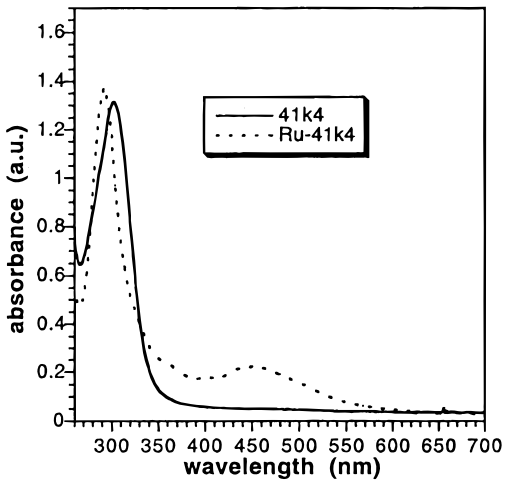

Figure 3. UV−vis absorption spectra of polyester **41k4** and its ruthenium complex in NMP solution.

Photoconductivity and Charge Mobility Measurements. The studies on photoconductivity and charge carrier mobilities were only carried out in polyamides because they formed higher quality films by solution casting. It is well-known that conjugated polymers have much higher carrier mobilities than those with a saturated polymer chain due to the delocalized π electrons.[28] Although the conjugation in polyamide is hampered by the presence of amide linkage, the free carriers are expected to migrate through the material via hopping process.[29] The polyamide ruthenium complexes are expected to exhibit higher photosensitivity charge carrier mobility because the [Ru(bpy)$_3$]$^{2+}$ species absorb strongly in the visible region. Moreover, they are able to act as extra charge carriers in the charge transport processes. This was shown in our previous examples of ruthenium-containing polymers.[15] Figure 10 shows the photocurrent response of different polyamide ruthenium complexes under an externally applied electric field. As the external electric field was increased, the photocurrent increased rapidly. The photoconductivity of the polymers appears to be dependent on the ruthenium content in the polymer. Under the same electric field strength, the conductivity

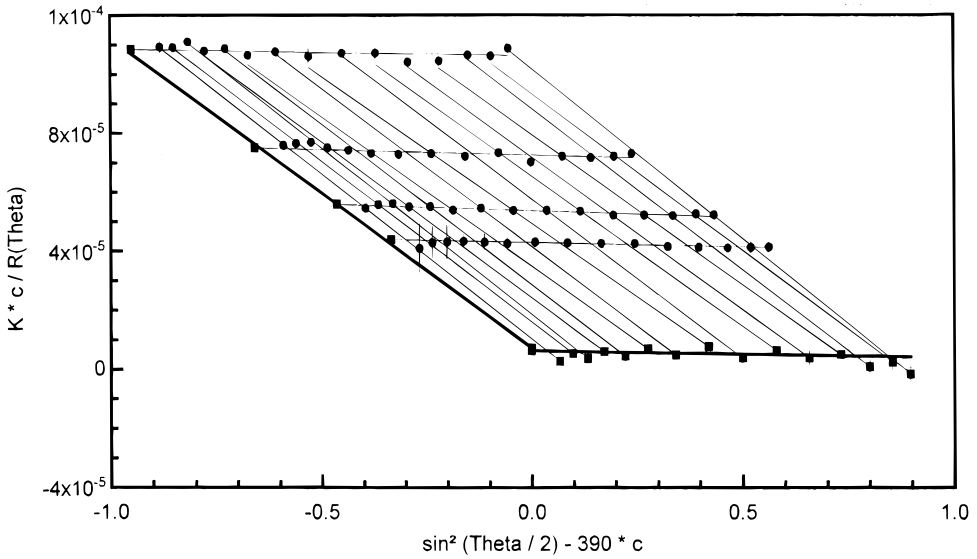

Figure 4. Zimm plot showing the light scattering from a sample of polyamide **17h** in 98% formic acid.

Table 4. Physical Data from the Light-Scattering Experiments for Some Polyamides

polymer	d*n*/d*c*	A_2 (mol mL/g^2)	M_w
17g	0.211	2.6×10^{-3}	23 000
17h	0.293	2.7×10^{-3}	39 000
17i	0.221	1.6×10^{-2}	26 500
17n	0.361	4.0×10^{-2}	27 500
Ru-17h	0.248	2.0×10^{-2}	151 000

increases as the ruthenium content is increased. This indicates that the ruthenium complexes play an important role in the photoconduction process by acting as the charge sensitizers.

The hole and electron transport properties were studied by the conventional time-of-flight (TOF) experiment. The charge transport processes were found to be dispersive in nature with a non-Gaussian carrier distribution across the polymer film. At room temperature, the hole and electron carrier mobilities of the metal-free polymers are on the order of 10^{-8} cm^2 V^{-2} S^{-1}. After the incorporation of ruthenium complexes to the polymer, the mobilities increased by 2−3 orders of magnitude, indicating that the ruthenium complexes provided extra charge carriers in the polymers.

Luminescence Properties. For the metal-free polyamides, the luminescence spectra were dominated by the emission band due to the aromatic ring systems. The photoluminescence (PL) spectra of polyamide **17i** in NMP solution and in the solid state are shown in Figure 11. The solution spectrum shows two emission bands centered at 450 and 494 nm, which are assignable to the $\pi^*-\pi$ emission of the diphenyl sulfone moiety. An intriguing feature was observed in the solid-state emission spectrum. The emission band was red-shifted compared to the solution spectrum. This is attributed to the emission from the exciplexes as a result of the formation of polymer aggregates in the solid state.[30]

After the incorporation of ruthenium, the PL spectra were dominated by the emission from the $[Ru(bpy)_3]^{2+}$ MLCT excited states (π^*-d). All polyamide ruthenium complexes showed an emission band centered at ca. 680−700 nm when excited at 370 or 500 nm. These observations indicate that the emissions from the MLCT states were not affected by changing the diamine monomers. In addition, it is interesting to note that the emission at 450−500 nm disappeared, possibly due to an energy transfer process in which the metal complexes quench the emission from the aromatic systems. The luminescence properties of the polyesters or the model ruthenium complexes are very similar to those of the polyamide analogues. The ruthenium bipyridyl complexes act as the luminophore and the emission due to the MLCT states was found at the vicinities of 700 nm.

It was shown previously that some ruthenium complexes or polymers could be fabricated into single-layer light-emitting devices.[11b] We investigated the light-emitting properties of some polyamides that can form good quality film. Figure 12 shows the current density−voltage curves of these devices at 298 K. It was observed that the turn-on voltage of the device decreased gradually when ruthenium content was increased, and polyamide **Ru-17b5** exhibits the lowest turn-on voltage at approximately 5 V. When the device was subjected to forward bias, red-orange emission was observed (Figure 13). The maximum luminance and the external quantum efficiencies η_{ext} of these devices were estimated to be approximately 100−120 cd/m^2 and 0.01%, respectively. The luminescence is tentatively assigned to be the π^*-d emission from the MLCT states of the ruthenium complexes. It was proposed that the light emission originated from an exciton with the characteristics of an excited $[Ru(bpy)_3]^{2+}$ species, which was formed by the recombination of hole and electron. The turn on voltage in the device was approximately 6 V, with maximum luminance and η_{ext} of approximately 91 cd/m^2 and 0.09%, respectively.

Conclusions

We have developed two series of polyamides and polyesters based on 2,2′-bipyridine-5,5′-dicarboxylic acid by using various polymerization methods. The synthetic condition and the formation of polymer−ruthenium complexes were studied. Thermotropic and lyotropic liquid crystal phases were also observed in some polymers. The phase transition temperatures depend on the rigidity of the main chain or the presence of flexible pendant groups. Because of the presence of ruthenium tris(2,2′-bipyridyl) typed complexes, the polymer−ruthenium complexes exhibited interesting photosensitization, charge transport, and light-emitting behaviors. The emission were dominated by the emission from

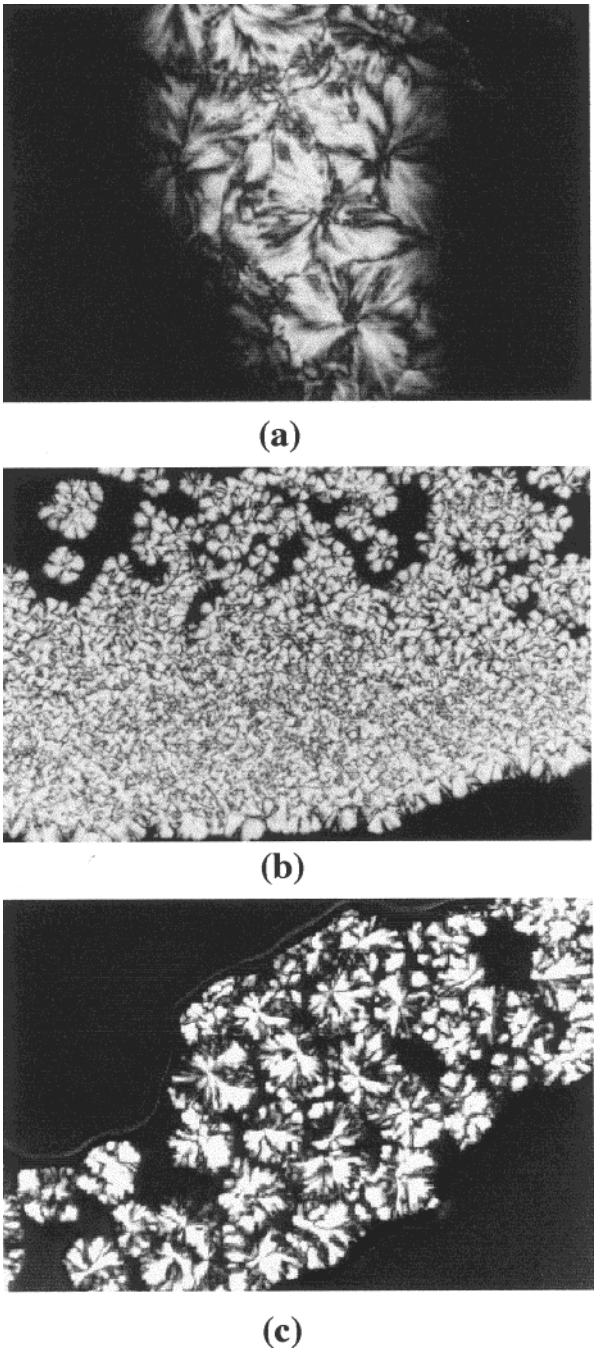

Figure 5. Optical polarized micrographs: (a) polyester **41m8** at 236 °C (400×); (b) polyester **41n** at 200 °C (200×); (c) ruthenium-containing polyamide **Ru-17b2** (4.4 wt % in HMPA−4% LiCl) at 25 °C (400×).

the MLCT states of the ruthenium complexes, which is probably a consequence of an energy transfer process from the polymer main chain to the metal complexes. In addition, some of these polymers were fabricated into single-layer EL devices, and they are potential candidates for light-emitting materials with high thermal stability.

Experimental Section

Materials. 1,4-Diaminobenzene (**3**), benzidine (**4**), 4,4′-diaminodiphenyl ether (**5**), 4,4′-diamino-3,3′-dimethoxybiphenyl (**7**), 4,4′-diaminostilbene-2,2′-disulfonic acid (**8**), 2,5-dibromo-1,4-diaminobenzene (**9**),[31] 1,5-diaminonaphthalene (**10**), 4,4′-diaminodiphenyl sulfone (**11**), 4,4′-methylenedianiline (**12**), 1,*n*-diaminoalkanes (**16a**−**c**, n = 3, 6, 12), 4,4′-dihydroxybiphenyl (**22**), bisphenol A (**23**), 4,4′-dihydoxybenzophone (**26**), dihydroxypropiophenone (**27**), 2,7-dihydroxynaphthalene (**28**), 1,n-dihydroxyalkane (**33a**−**i**, n = 2, 4, 5, 6, 7, 8, 9, 10, 12), 2,2-dimethyl-1,3-propanediol (**36**), 2,5-dihydroxybenzoquinone, and 6-chloro-1-hexanol were purchased from Lancaster Synthesis Ltd. 4,4′-(Hexafluoroisopropyliene)dianiline **6**, 4,4′-ethylenedi-*m*-toluidine (**15**), 4,4′-(hexafluoroisopropyliene)-diphenol (**24**), 2,2-dimethyl-1,3-propanediol (**35**), 2-methyl-2-propyl-1,3-propanediol (**37**), and 2-butyl-2-ethyl-1,3-propanediol (**38**) were purchased from Aldrich Chemical Co. Inc. 2,2′-Bipyridine-5,5′-dicarboxylic acid (**1**), 2,2′-bipyridine-4,4′-dicar-

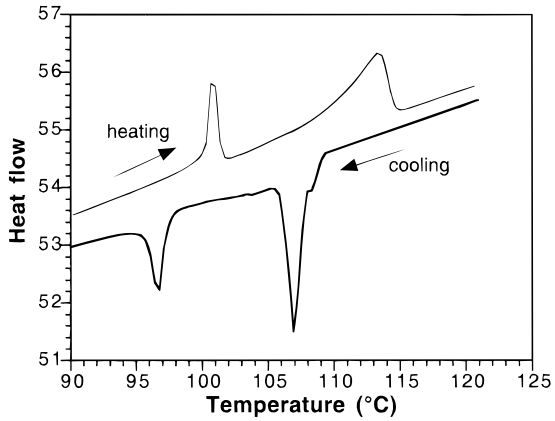

Figure 6. DSC thermogram of polymer **41h2** with heating and cooling rates of 10 °C/min.

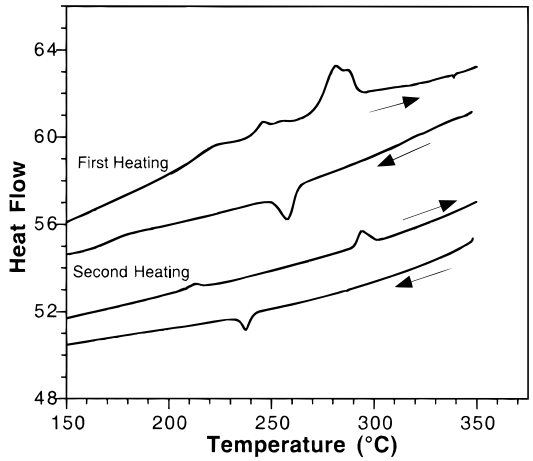

Figure 7. First and second DSC scans of polymer **41k2** with heating and cooling rates of 10 °C/min.

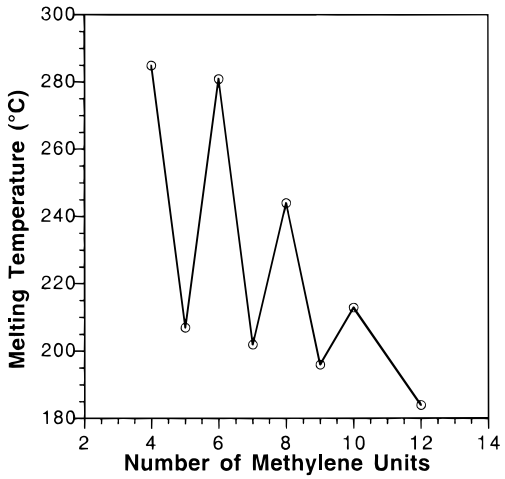

Figure 8. Variation of melting temperature with the number of methylene units on the main chain for polyesters **41m2**−**m9**.

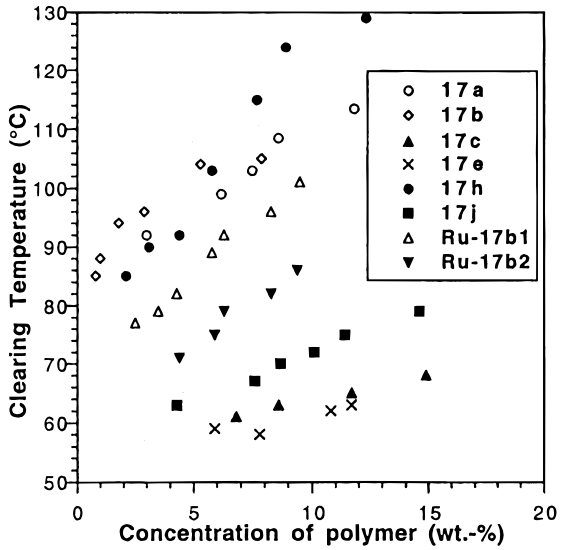

Figure 9. Plot of the clearing temperature vs concentration (% w/w) for different polyamides and their ruthenium complexes in HMPA−4% LiCl solution.

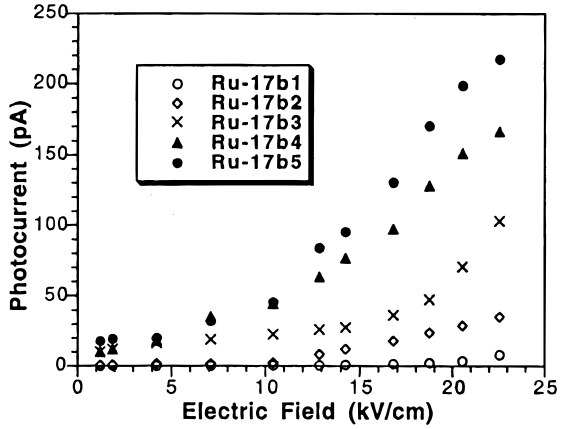

Figure 10. Photocurrent response of different polyamide ruthenium complexes as a function of externally applied electric field.

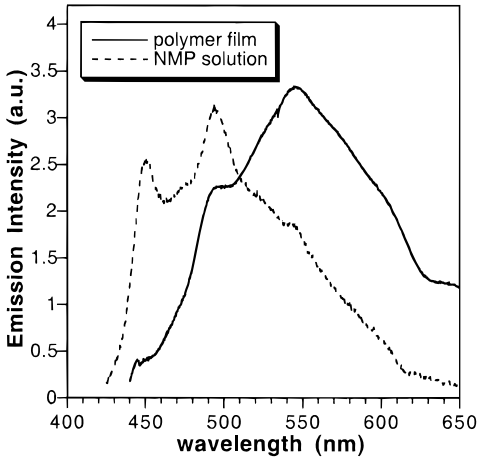

Figure 11. Photoluminescence spectra of polyamide **17i** in NMP solution and in the solid state excited at 330 nm.

boxylic acid (**2**),[32] 1,*n*-bis(*n*-aminophenoxy)alkanes[33] (**13a**−**e**
14, $n = 4, 6, 8, 10, 12$), *cis*-dichlorobis(2,2′-bipyridine)ruthenium(II) dihydrate, $Ru(bpy)_2Cl_2 \cdot 2H_2O$, and *cis*-$[Ru(bpy)_2(acetone)_2](OTf)_2$[34] were synthesized as described in the literature. Hexamethylphosphoramide (HMPA) was distilled over CaH_2 under reduced pressure. Triphenyl phosphite (Lancaster) was distilled under reduced pressure. Pyridine was

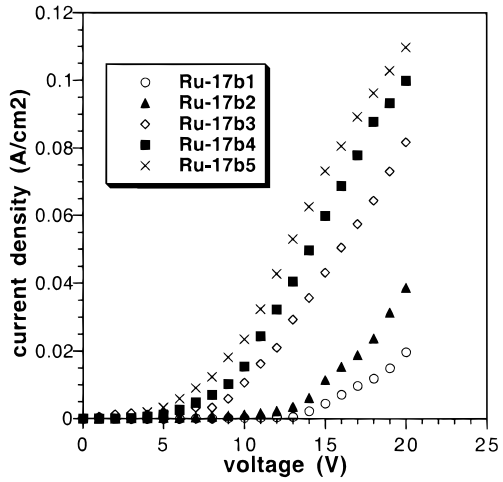

Figure 12. Current−voltage characteristics of the EL devices fabricated from various polyamide ruthenium complexes.

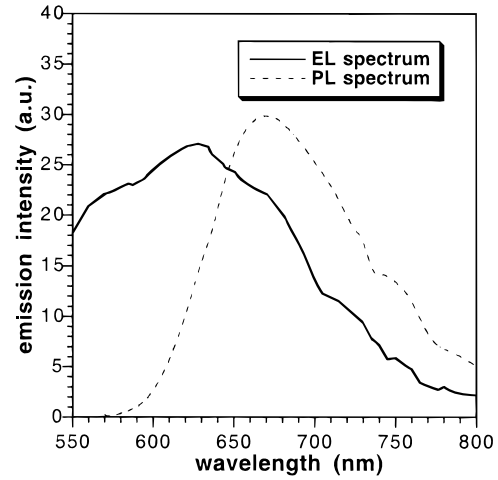

Figure 13. Photo- and electroluminescence spectra of the polyamide ruthenium complex **Ru-17b5**. The EL spectrum was collected under a forward bias of 20 V.

distilled over CaH_2 prior to use. Unless otherwise specified, all the reagents were used as received without further purification.

Instruments. ^1H and ^{13}C NMR spectra were collected on a Bruker 300 DPX NMR spectrometer. FTIR spectra (KBr pellet) were collected on a Bio-Rad FTS-7 FTIR spectrometer. Mass spectrometry was performed on a high-resolution Finnigan MAT-95 mass spectrometer. Thermal analyses were performed on Perkin-Elmer DSC7 and TGA7 thermal analyzers with a heating rates of 10 and 15 °C/min, respectively. The polarized microscope observation was performed on a Leica DMR microscope equipped with a Leitz microscope heater. The viscosity measurements were performed in a constant-temperature bath (30 °C) using an Ubbelohde viscometer, with a solution concentration of 0.5 g/dL in an appropriate solvent. The weight-average molecular weights of the polymers were determined with a Wyatt Technology DAWN DSP laser photometer equipped with a He−Ne laser (632.8 nm). The refractive index increment (d*n*/d*c*) was measured with a Viscotek 250 viscosity/refractive index detector using an aqueous sodium chloride solution as the reference standard. For the determination of metal content in polymers, the polymer samples were digested in refluxing concentrated HNO_3 for 3 h, and the concentration of ruthenium in the resulting solution was determined with a Carl Zeiss Plasmaquant 110 emission spectrometer.

Ruthenium Complexes Ru-1 and Ru-2. They were prepared according to the literature procedure.[35] **Ru-1.** Yield: 83%. ^1H NMR (DMSO-d_6), δ: 9.02 (d, $J = 8.3$ Hz, 2 H), 8.87

(dd, J = 8.2, 12.1 Hz, 4 H), 8.54 (dd, J = 1.65, 8.35 Hz, 2 H), 8.20 (m, 4 H), 8.01 (d, J = 1.5 Hz, 2 H), 7.53 (dd, J = 5.07, 20.72 Hz, 4 H), 7.55 (m, 4 H). ^{13}C NMR (DMSO-d_6), δ: 163.81, 158.57, 156.57, 156.07, 151.88, 151.29, 138.10, 130.31, 127.86, 125.38, 124.06. FABMS, *m/e*: 803 ($M^+ - PF_6$); $C_{32}H_{24}N_6O_4F_6$-PRu requires 802.61.

Ru-2. Yield: 85%. ^{1}H NMR (DMSO-d_6), δ: 9.25 (s, 2 H), 8.24 (d, J = 5.78 Hz, 4 H), 8.19 (m, 4 H), 7.95 (d, J = 5.82 Hz, 2 H), 7.88 (dd, J = 1.48, 5.83, 2 H), 7.73 (dd, J = 5.49, 12.10 Hz, 4 H), 7.62 (m, 4 H). ^{13}C NMR (DMSO-d_6), δ: 164.84, 157.12, 156.15, 152.10, 151.42, 150.87, 139.15, 138.20, 127.89, 124.39, 124.06. FABMS, *m/e*: 803 ($M^+ - PF_6$); $C_{32}H_{24}N_6O_4F_6$-PRu requires 802.61.

Bis(4-aminophenoxy)alkanes (13a−e, *n* = 4, 6, 8, 10, 12). They were synthesized by three-step processes starting from 4-acetamidophenol with the corresponding 1,*n*-dibromoalkane. The synthesis of 1,6-bis(4-aminophenoxy) hexane (**13b**) is described as the general procedure. A mixture of 4-acetamidophenol (8.16 g, 54 mmol), potassium hydroxide (3 g, 54 mmol), ethanol (50 mL), and water (15 mL) was heated under reflux in a 100 mL round-bottom flask. 1,6-Dibromohexane (5.9 g, 24 mmol) was added to the mixture dropwise, and the solution was heated under reflux for 24 h. Upon cooling, the white precipitate was filtered and washed with water. The product was recrystallized from ethanol. Concentrated hydrochloric acid (20 mL) and ethanol (30 mL) were then added to the resulting 1,6-bis(4-acetamidophenoxy)-hexane (3.8 g, 10 mmol) and the mixture was heated under reflux for 4 h. The crystalline, yellow precipitate was filtered, washed with ethyl acetate, and dried in a vacuum oven for 12 h. A suspension of the resulting 1,6-bis(4-aminophenoxy)-hexane dihydrochloride (1.9 g, 5 mmol) in water (50 mL) was prepared in a 100 mL flask at room temperature. Potassium carbonate (1.52 g, 1.1 mmol) in water (10 mL) was added to the suspension. The final product, 1,6-bis(4-aminophenoxy)-hexane (**13b**) was separated as white powder after stirring for 5 min. The crude product was treated with activated carbon and recrystallized from water−ethanol (3:2) mixture to yield fine needle-shaped crystals (yield 70%).

Synthesis of Polyamides 17a−p. The synthesis of polyamide **17c** is described as the general procedure. A mixture of 4,4′-diaminodiphenyl ether (**5**) (0.20 g, 1 mmol), 2,2-bipyridine-5,5′-dicarboxylic acid (**1**) (0.24 g, 1 mmol), triphenyl phosphite (0.55 mL, 2.1 mmol), lithium chloride (0.52 g), pyridine (3 mL), and HMPA (10 mL) was added to a 25 mL, two-necked round-bottom flask under a nitrogen atmosphere. The reaction mixture was stirred at the appropriate temperature for 24 h. The viscous solution was poured into rapidly stirred methanol. The polymer collected was purified by extraction with methanol and then dried under vacuum at 100 °C for 1 day.

Model Ruthenium Complexes Ru-1 and Ru-2. The synthesis of complex **Ru-1** is described as the general procedure. A mixture of 2,2′-bipyridine-5,5′-dicarboxylic acid (**1**) (0.82 g, 1 mmol), *p*-toluidine (0.21 g, 2 mmol), triphenyl phosphite (0.55 mL, 2.1 mmol), lithium chloride (0.52 g, 12 mmol), pyridine (3 mL), and HMPA (10 mL) was added to a 25 mL two-necked round-bottom flask under nitrogen atmosphere. The reaction mixture was stirred at 100 °C for 48 h. The viscous solution was poured into rapidly stirred methanol. The complex was purified by dissolving in acetone and then reprecipitated in diethyl ether. Yield: 87%. Mp: 330 °C dec. FTIR (KBr): ν = 3040 cm^{-1} (aromatic CH), 1654 cm^{-1} (C═O stretching), 1592 cm^{-1} (C═N stretching), 840 cm^{-1} (P−F stretching). ^{1}H NMR (DMSO-d_6), δ: 10.48 (s, 2 H), 9.07 (d, J = 8.22 Hz, 2 H), 8.86 (d, J = 6.59 Hz, 4 H), 8.73 (d, J = 8.19 Hz, 2 H), 8.20 (dd, J = 8.40, 16.97 Hz, 4 H), 8.07 (s, 4 H), 7.58 (m, 8 H), 7.16 (d, J = 7.79 Hz, 4 H), 2.08 (s, 6 H). ^{13}C NMR (DMSO-d_6), δ: 160.92, 157.63, 156.60, 156.35, 151.62, 151.36, 150.94, 138.04, 135.91, 135.59, 133.44, 129.09, 127.79, 124.55, 120.45, 20.40. FABMS, *m/e:* 981 ($M^+ - PF_6$); $C_{46}H_{38}N_8O_2F_6$-PRu requires 980.89.

Ru-2. Yield: 85%. Mp: 334 °C dec. FTIR (KBr): ν = 3035 cm^{-1} (aromatic CH stretching), 1655 cm^{-1} (C═O stretching), 1594 cm^{-1} (C═N stretching), 840 cm^{-1} (P−F stretching). ^{1}H NMR (DMSO-d_6), δ: 10.74 (s, 2 H), 9.45 (s, 2 H), 9.07 (s, 2 H), 8.86 (d, J = 5.77 Hz, 4 H), 8.18 (m, 4 H), 7.94 (s, 4 H), 7.78 (d, J = 5.32 Hz, 2 H), 7.73 (d, J = 4.83 Hz, 2 H), 7.65 (d, J = 8.37 Hz, 2 H), 7.53 (dd, J = 6.40, 14.49 Hz, 4 H) 7.19 (d, J = 8.38 Hz, 4 H), 2.27 (s, 6 H). ^{13}C NMR (DMSO-d_6), δ: 156.85, 156.31, 156.19, 151.84, 151.31, 142.72, 138.23, 135.44, 133.87, 129.23, 127.95, 125.70, 124.44, 122.30, 120.60, 20.42. FABMS, *m/e:* 981 ($M^+ - PF_6$); $C_{46}H_{38}N_8O_2F_6$PRu requires 980.89.

Synthesis of Polymer−Ruthenium Complexes. The polymer−ruthenium complexes were synthesized by polymerizing the ruthenium-containing monomer **Ru-1** with the diamine monomers (method A) or by the metalation of the metal-free polyamides (method B). The general procedures are described below.

Method A. The synthesis of polymer **Ru-17b2** is described as the general procedure. A mixture of **Ru-1** (0.41 g, 0.5 mmol), 2,2′-bipyridine-5,5′-dicarboxylic acid (**1**) (0.12 g, 0.5 mmol), benzidine (**4**) (0.02 g, 0.1 mmol), triphenyl phosphite (0.55 mL, 2.1 mmol), lithium chloride (12 mmol 0.52 g), pyridine (3 mL), and HMPA (10 mL) were added into a 25 mL two-necked round-bottom flask under a nitrogen atmosphere. The reaction mixture was stirred at 100 °C for 48 h. The viscous solution was poured into rapidly stirred methanol. The polymer−ruthenium complex was purified by extraction with methanol and then dried in a vacuum at 100 °C for 1 day.

Method B. A mixture of polyamide **17b** (0.32 g) and Ru(bpy)$_2$(OTf)$_2$ (acetone)$_2$ (0.72 g, 1 mmol) was refluxed in DMF (10 mL) for 48 h under a nitrogen atmosphere. The resulting mixture was poured into methanol and the precipitates were filtered and washed with DMF and methanol. The product was dried in a vacuum at 80 °C for 1 day.

Synthesis of Monomers for Polyesters. 2,2′-Bipyridine-5,5′-dicarbonyl chloride (20). A mixture of 2,2′-bipyridine-5,5′-dicarboxylic acid **1** (1 g, 4.1 mmol), thionyl chloride (20 mL), and pyridine (0.1 mL) was refluxed for 24 h. The excess thionyl chloride was removed by distillation and the crude product was recrystallized with *n*-heptane. Yield: 82%.

Diethyl-2,2′-bipyridine-5,5′-dicarboxylate (21). A mixture of 2,2′-bipyridine-5,5-dicarboxylic acid (**1**) (3 g, 12.29 mmol), ethanol (50 mL), and concentrated sulfuric acid (3 mL) was refluxed for 24 h. The reaction mixture was poured into ice−water mixture and the precipitate was filtered. The product was recrystallized from 95% ethanol to yield white crystals. Yield: 75%. Mp: 151 °C. FTIR (KBr): ν = 1762 cm^{-1} (C═O stretching), 1601 cm^{-1} (C═N stretching). ^{1}H NMR (DMSO-d_6), δ: 9.21 (s, 2 H), 8.59 (dd, J = 6.3, 1.5 Hz, 2 H), 8.48 (dd, J = 8.3, 2.1 Hz, 2 H), 4.39 (q, J = 7.1 Hz, 2 H), 1.37 (t, J = 7.1 Hz, 3 H). ^{13}C NMR (DMSO-d_6), δ: 157.3, 149.9, 138.25, 126.3, 124.1, 121.1, 61.3, 14.0. MS, *m/e*: 300.111007; $C_{16}H_{16}O_4N_2$ requires 300.111006.

2,5-Dialkoxy-1,4-dihydroxybenzenes (29a−c). They were prepared from 2,5-dihydroxyebnzoquinone in two steps.[24] The synthesis of 2,5-didecoxy-1,4-dihydroxybenzene (**29a**) is described as the general procedure. A mixture of 2,5-dihydroxy-1,4-benzoquinone (5 g, 36 mmol), *n*-decanol (10 g, 0.3 mol), boron trifluoride etherate (9 mL, 72 mmol), and THF (50 mL) were heated at 60 °C for 3 h. The crude product was obtained by cooling the reaction mixture to −20 °C. It was washed with hexane and recrystallized from THF. The resulting product, 2,5-didecoxy-1,4-benzoquinone (2.67 g, 5.6 mmol), was dissolved in chloroform (60 mL) and then added to sodium hydrosulfite (19.1 g, 0.1 mol) in water (100 mL). The mixture was stirred for 20 h at room temperature. During the course of the reaction, the red color disappeared when the product precipitated. The product was recrystallized from hexane and collected as white needle-shaped crystals.

2,5-Didecoxy-1,4-dihydroxybenzenes (29a). Yield: 59%. ^{1}H NMR ($CDCl_3$), δ: 6.56 (s, 2 H), 5.25 (s, 2 H), 3.95 (t, J = 6.5 Hz, 4 H), 1.77 (m, 4 H), 1.27 (m, 28 H), 0.88 (t, J = 6.3 Hz, 6 H). ^{13}C NMR ($CDCl_3$), δ: 139.20, 138.69, 100.64, 69.82, 31.84, 29.82, 29.64, 29.60, 29.41, 29.14, 22.84, 14.32. MS, *m/e*: 422.339610; $C_{26}H_{46}O_4$ requires 422.339610.

2,5-Didodecoxy-1,4-dihydroxybenzenes (29b). Yield: 59%. ^{1}H NMR ($CDCl_3$), δ: 6.59 (s, 2 H), 5.26 (s, 2 H), 3.95 (t, J = 6.6 Hz, 4 H), 1.79 (m, 4 H), 1.26 (m, 36 H), 0.88 (t, J = 6.7 Hz, 6 H). ^{13}C NMR ($CDCl_3$), δ: 139.52, 138.74, 100.58, 69.77,

31.93, 29.66, 29.64, 29.60, 29.38, 29.31, 26.01, 22.70, 14.14. MS, *m/e*: 478.402211; $C_{30}H_{54}O_4$ requires 478.402211.

2,5-Dihexadecoxy-1,4-dihydroxybenzenes (29c). Yield: 60%. ^{1}H NMR ($CDCl_3$), *δ:* 6.56 (s, 2 H), 5.25 (s, 2 H), 3.94 (t, $J = 6.6$ Hz, 4 H), 1.77 (m, 4 H), 1.26 (m, 52 H), 0.88 (t, $J = 6.7$ Hz, 6 H). ^{13}C NMR ($CDCl_3$): *δ,* 139.60, 138.81, 100.59, 70.01, 31.95, 29.72, 29.66, 29.64, 29.61, 29.39, 26.02, 22.72, 14.15. MS, *m/e*: 590.527411; $C_{38}H_{70}O_4$ requires 590.527412.

4,4′-Bis(6-hydroxyhexoxy)biphenyl (30). A mixture of 4,4′-dihydroxybiphenyl **22** (0.93 g, 5 mmol), 6-chloro-1-hexanol (1.64 g, 12 mmol), and potassium carbonate (8.30 g, 60 mmol) in DMF (10 mL) was refluxed for 12 h. The reaction mixture was poured into excess water. The precipitate was washed with diluted hydrochloric acid and then thoroughly with water. The crude product was recrystallized twice from chloroform and dried at 40 °C for 1 day in a vacuum. Yield: 64%. Mp: 177 °C. ^{1}H NMR (DMSO-d_6), *δ:* 7.51 (d, $J = 8.7$ Hz, 4 H) 6.97 (d, $J = 8.8$ Hz, 4 H), 4.38 (s, 2 H), 3.98 (t, $J = 6.4$ Hz, 4 H), 3.40 (t, $J = 6.1$ Hz, 4 H), 1.72 (m, 4 H), 1.38 (m, 12 H). ^{13}C NMR (DMSO-d_6), *δ:* 158.61, 133.04, 128.02, 115.64, 68.28, 61.49, 33.34, 29.62, 26.30, 26.14. MS, *m/e*: 386.245709; $C_{24}H_{34}O_4$ requires 386.246709.

1,*n*-Bis(4-hydroxyphenoxy)alkanes (32a−d, *n* = 6, 8, 10, 12). The synthesis of monomer **32d** is described as the general procedure. In a 500 mL three-necked round-bottom flask, sodium hydrosulfite (0.03 g) in 95% ethanol (30 mL) was deaerated with nitrogen. Hydroquinone (16.96 g, 0.154 mol), 1,12-dibromododecane (5.1 g. 15.4 mmol) were added with stirring, and the solution was heated under reflux for 30 min. A solution of potassium hydroxide (2.58 g, 46 mmol) in 95% ethanol (15 mL) was added. The mixture was heated under reflux for another 5 h under a nitrogen atmosphere. After cooling to room temperature, the solution was acidified with 30% sulfuric acid (30 mL), and then ethanol (60 mL) was added. The solid was filtered and washed with water and hot petroleum ether (3 × 20 mL). The product was recrystallized from ethanol, and the final product was dried under vacuum at 40−60 °C for 1 day.

1,6-Bis(4-hydroxyphenoxy)hexane (32a). Yield: 41%. ^{1}H NMR (DMSO-d_6), *δ:* 8.86 (s, 2 H), 6.73 (d, $J = 9.0$ Hz, 4 H), 6.65 (d, $J = 9.0$ Hz, 4 H), 3.33 (t, $J = 7.1$ Hz, 4 H), 1.67 (m, 4 H), 1.43 (m, 4 H). ^{13}C NMR (DMSO-d_6), *δ:* 152.30, 151.86, 116.50, 116.17, 68.60, 29.65, 26.21. MS, *m/e*: 302.151810; $C_{20}H_{26}O_4$ requires 302.151809.

1,8-Bis(4-hydroxyphenoxy)octane (32b). Yield: 40%. ^{1}H NMR (DMSO-d_6), *δ:* *δ* 8.87 (s, 2 H), 6.72 (d, $J = 9.0$ Hz, 4 H), 6.64 (d, $J = 9.0$ Hz, 4 H), 3.83 (t, $J = 6.4$ Hz, 4 H), 1.65 (m, 4 H), 1.34 (m, 4 H). ^{13}C NMR (DMSO-d_6), *δ:* 151.90, 150.97, 115.60, 115.23, 67.52, 28.32, 25.73. MS, *m/e*: 330.183110; $C_{20}H_{26}O_4$ requires 330.183110.

1,10-Bis(4-hydroxyphenoxy)decane (32c). Yield: 42%. ^{1}H NMR (DMSO-d_6), *δ:* *δ* 8.87 (s, 2 H), 6.72 (d, $J = 9.0$ Hz, 4 H), 6.64 (d, $J = 9.0$ Hz, 4 H), 3.82 (t, $J = 7.0$ Hz, 4 H), 1.66 (m, 4 H), 1.37 (m, 12 H). ^{13}C NMR (DMSO-d_6), *δ:* 151.63, 150.91, 115.54, 115.18, 67.67, 28.74, 25.45. MS, *m/e*: 358.214409; $C_{22}H_{30}O_4$ requires 358.214410.

1,12-Bis(4-hydroxyphenoxy)dodecane (32d). Yield: 48%. ^{1}H NMR (DMSO-d_6), *δ:* *δ* 8.86 (s, 2 H), 6.73 (d, $J = 9.0$ Hz, 4 H), 6.65 (d, $J = 9.0$ Hz, 4 H), 3.33 (t, $J = 7.1$ Hz, 4 H), 1.67 (m, 4 H), 1.43 (m, 16 H). ^{13}C NMR (DMSO-d_6), *δ:* *δ* 152.30, 151.86, 116.50, 116.17, 68.60, 29.65, 26.21. MS, *m/e*: 386.246710; $C_{24}H_{34}O_4$ requires 386.246710.

2-Hydroxymethyl-1-nonanol (34). Sodium metal (4.74 g, 0.206 mol) was added gradually to absolute ethanol (100 mL). After the reaction was complete, diethyl malonate (30 g, 0.187 mol) was added slowly through an addition funnel. 1-Bromooctane (36.17 g, 0.187 mmol) was added to the solution dropwise. The reaction mixture was refluxed for 24 h, and the solvent was removed under reduced pressure. The residue was extracted with diethyl ether (3 × 25 mL), and the combined organic layer was washed with water (3 × 50 mL). After removal of the solvent, the crude product was distilled under vacuum, and the product 2-octyldiethylmalonate was obtained as a colorless liquid (bp 116−120 °C, 0.1 mbar). Yield: 68%. ^{1}H NMR ($CDCl_3$), *δ:* 7.51 (d, $J = 8.7$ Hz, 4 H), 6.97 (d, $J = 8.8$ Hz, 4 H), 4.38 (s, 2 H), 3.98 (t, $J = 6.4$ Hz, 4 H), 3.40 (t, $J = 6.1$ Hz, 4 H), 1.72 (m, 4 H), 1.38 (m, 12 H). ^{13}C NMR (DMSO-d_6), *δ:* 169.60, 61.23, 52.18, 31.92, 29.38, 29.32, 29.29, 28.83, 27.41, 22.74, 14.14. MS, *m/e*: 272.198759; $C_{15}H_{28}O_4$ requires 272.198759. A solution of 2-octyldiethylmalonate (3 g, 15.9 mmol) in anhydrous THF (30 mL) was added to a stirred suspension of $LiAlH_4$ (1.4 g, 38.2 mmol) in anhydrous THF (30 mL) at 0 °C. The resulting mixture was stirred for 24 h at room temperature and then refluxed for 3 h. Saturated NH_4Cl solution was then added to reaction mixture at 0 °C until no more hydrogen gas evolved. The solution was extracted with $CHCl_3$ (3 × 50 mL). The combined organic layer was dried over magnesium sulfate. After removal of the solvent, the product was recrystallized from EtOH/H_2O (7:3) and white crystals were obtained. Yield: 63%. ^{1}H NMR ($CDCl_3$), *δ:* 3.81 (dd, $J = 10.6$, 3.7 Hz, 2 H), 3.64 (dd, $J = 10.6$, 7.7 Hz, 2 H), 2.62 (s, 2 H), 2.18 (m, 1 H), 1.27 (m,14 H), 0.88 (t, $J = 6.5$ Hz, 3 H). ^{13}C NMR, *δ:* 66.68, 41.93, 31.88, 29.90, 29.51, 29.30, 27.71, 27.24, 22.68, 14.12. MS, *m/e*: 188.177630; $C_7H_{16}O_2$ requires 188.177629.

Model Compound 39. Under a nitrogen atmosphere, a mixture of 2,2′-bipyridine-5,5-dicarbonyl chloride (**20**) (0.20 g, 0.71 mmol) and 4-methoxyphenol (0.26 g, 2.1 mmol) in dry pyridine (20 mL) was refluxed for 24 h. The solution was poured into methanol (100 mL). The solid was filtered and recrystallized with DMF. Yield: 81%. Mp: 219 °C. FTIR (KBr): $\nu = 1739$ cm^{-1} (C═O stretching), 1603 cm^{-1} (C═N stretching). ^{1}H NMR (DMSO-d_6), *δ:* 9.40 (s, 2 H), 8.68 (m, 4 H), 7.28 (d, $J = 9.0$ Hz, 4 H), 7.03 (d, $J = 9.1$ Hz, 4 H), 3.80 (s, 6 H). ^{13}C NMR (DMSO-d_6), *δ:* 166.66, 164.31, 158.66, 157.84, 150.97, 139.20, 127.78, 126.40, 123.36, 121.96, 115.19, 56.13. MS *m/e*: 456.132136; $C_{26}H_{20}O_6N_2$ requires 456.132137.

Synthesis of Polyesters. The polyesters were synthesized by either alcoholysis of acid chloride (method C) or by transesterification (method D). Those polyesters derived from rigid aromatic diols (polymers **41a**−**41h3**) were synthesized by polycondensation between the diacid chloride **20** and the corresponding diol monomers (**22**−**29c**) in pyridine solution. On the other hand, those polyesters with more flexible main chain (polymers **41i**−**41s**) were synthesized by transesterfication reaction between monomer **21** and the corresponding diol monomers (**30**−**38**) catalyzed by titanium(IV) isopropoxide.

Synthesis of Polyesters 41a-41h3 by Alcoholysis of Diols. The synthesis of polymer **41h2** was described as the general procedure. A mixture of 2,2′-bipyridine-5,5′-dicarbonyl chloride (**20**) (0.20 g, 0.71 mmol) and 2,5-didodecoxy-1,4-dihydroxybenzene (**29b**) (0.42 g, 0.71 mmol) in dry pyridine (20 mL) was refluxed under a nitrogen atmosphere for 24 h. During the course of the reaction, the solution became homogeneous. The reaction mixture was poured into excess methanol (200 mL). The polymer was filtered and purified by washing in a Soxhlet extractor for 1 day. It was dried under vacuum at 80 °C for 1 day.

Synthesis of Polyesters 41i−41s by Transesterification. The synthesis of polymer **41i** was described as the general procedure. A mixture of 5,5′-diethyl-2,2′-bipyridine dicarboxylate (**21**) (0.018 g, 0.05 mmol), 4,4′-bis(6-hydroxyhexoxy)biphenyl (**30**) (0.019 g, 0.05 mmol), and titanium(IV) isopropoxide (1 mg) were heated in a 25 mL round-bottom flask under nitrogen with an initial temperature of 165 °C (10−20 °C higher than the melting points of the diol or diester monomers). The temperature was maintained at 165 °C for 2 h, and the reaction mixture became very viscous. The temperature was increased until the reaction mixture melted. When the mixture solidified, the temperature was gradually increased again. Finally, the temperature was kept at 250 °C under vacuum for 2 h. After the mixture was cooled, hot 1,1,2,2-tetrachlorethane (30 mL) was added. The solution was poured into methanol (200 mL), and the polymer was filtered, washed thoroughly with water, andextracted with methanol in a Soxhlet extractor for 1 day. It was dried at 80 °C under vacuum for 2 days.

Polyester Ruthenium Complexes. The synthesis of polymer metal complex **Ru-41k4** is described as the general

procedure. Under a nitrogen atmosphere, *cis*-[Ru(bpy)$_2$(acetone)$_2$]-(OTf)$_2$ (0.14 g, 0.17 mmol) was added to a solution of polymer **41k4** (0.1 g) in NMP solution (25 mL). The solution was heated at 120 °C for 24 h. After cooling, an aqueous solution of KPF_6 was added and the precipitate was collected by filtration. The resulting solid was washed with water/methanol thoroughly and dried under reduced pressure at 100 °C for 1 day.

Model Complex 40. Under a nitrogen atmosphere, a mixture of *cis*-[Ru(bpy)$_2$(acetone)$_2$](OTf)$_2$ (0.36 g, 0.45 mmol), compound **39** (0.19 g, 0.45 mmol), and NMP (20 mL) were stirred at 120 °C for 24 h. The reaction mixture was precipitated in an aqueous solution of KPF_6. The solid obtained was washed thoroughly with water, redissolved in CH_3CN, and reprecipitated in diethyl ether. The reddish brown solid was dried under reduced pressure at 100 °C for 1 day. Yield: 81%. FTIR (KBr): $\nu = 1741$ cm^{-1} (C=O stretching), 1604 cm^{-1} (C=N stretching), 842 cm^{-1} (P−F stretching). ^{1}H NMR ($CDCl_3$), *δ:* 9.03 (d, $J = 8.0$ Hz, 2 H), 8.86 (m, 4 H), 8.72 (d, $J = 7.9$ Hz, 2 H), 8.20 (m, 4 H), 8.05 (s, 2 H), 7.89 (d, $J = 5.2$ Hz, 2 H), 7.81 (d, $J = 5.1$ Hz, 2 H), 7.58 (d, $J = 6.4$ Hz, 2 H), 7.52 (d, $J = 5.2$ Hz, 2 H), 7.09 (d, $J = 9.0$ Hz, 4 H). 6.97 (d, $J = 8.9$ Hz, 4 H), 3.74 (s, 6 H). ^{13}C NMR (DMSO-d_6), *δ:* 161.64, 159.59, 157.16, 156.63, 156.55, 156.20, 151.44, 143.27, 138.17, 128.57, 127.86, 124.42, 122.15, 114.42, 55.38. FABMS, *m/e*: 1015 ($M^+ - PF_6$); $C_{46}H_{36}O_6N_6F_6PRu$ requires 1014.86.

Physical Characterizations. The polymer films for photoconductivity and charge mobility measurements were prepared by casting a polymer solution onto an indium−tin−oxide coated glass slide and the solvent was evaporated slowly. The typical thickness of the polymer film was approximately 1 μm. A thin layer of gold electrode (100 Å) was coated on the polymer film surface by thermal evaporation under high vacuum (10^{-6} mbar). For EL measurements, the polymer films were prepared by spin coating the polymer solution onto ITO glass. A 4 × 5 array of aluminum electrodes (diameter = 4 mm, thickness = 100 nm) was deposited on the polymer film by thermal evaporation. A forward bias was applied to the light-emitting diode and the current−voltage characteristics were studied by a Keithley 2400 sourcemeter. The photoluminescence (PL) and electroluminescence (EL) spectra were collected on an ORIEL MS-257 monochromator equipped with an ANDOR DV420−BV charge-coupled device (CCD) detector. For the photoconductivity measurements, a Laser Physics Reliant 300 argon-ion laser (488 nm) was used as the light source. The incident light was modulated with a mechanical chopper and the resulting photocurrent was monitored with a Standard Research System SR 510 lock-in amplifier. The charge carrier mobilities were determined by the conventional time-of-flight experiment.[36] A Laser Science VSL-337 nitrogen laser was used to generated pulsed laser source [wavelength = 337.1 nm, pulse energy = 120 μJ, and pulse width full width at half-maximum (fwhm) = 3 ns]. The transient photocurrent was monitored by an oscilloscope.

Acknowledgment. The worked described in this paper was substantially supported by The Research Grants Council of The Hong Kong Special Administrative Region, China (Project Nos. HKU 495/96P and HKU 7093/97P). Partial financial support from the University Research Grant (University of Hong Kong) is also acknowledged. We also thank Mr. Cheuk Fung Chau and Dr. Wing Tat Chan for their assistance in the ICP experiments.

References and Notes

(1) (a) Juris, A.; Balzani, V.; Barigelletti, F.; Campagna, S.; Belser, P.; Von Zelewsky, A. *Coord. Chem. Rev.* **1988**, *84*, 85. (b) Kalyanasundaram, K. *Coord. Chem. Rev* **1982**, *46*, 159.

(2) Sauvage, J.-P.; Collin, J.-P.; Chambron, J.-C.; Guillerez, S.; Coudret, C.; Balzani, V.; Barigelletti, F.; De Cola, L.; Flamigni, L. *Chem. Rev.* **1994**, *94*, 993.

(3) (a) Card, R. J.; Neckers, D. C. *Inorg. Chem.* **1978**, *17*, 2345. (b) Kurimura, Y.; Shinozaki, N.; Ito, F.; Uratani, Y.; Shigehara, K.; Tsuchida, E.; Kaneko, M.; Yamada, A. *Bull. Chem. Soc. Jpn.* **1982**, *55*, 380. (c) Kaneko, M.; Ochiai, M.; Kunosita, K.; Yamada, A. *J. Polym. Sci., Polym. Chem. Ed.* **1982**, *20*, 1011.

(4) Cosnier, S.; Deronzier, A.; Roland, J.-F. *J. Electroanal. Chem.* **1990**, *285*, 133.

(5) (a) Yamamoto, T.; Yoneda, Y.; Maruyama, T. *J. Chem. Soc., Chem. Commun.* **1992**, 1652. (b) Maruyama, T.; Kutoba, K.; Yamamoto, Y. *Macromolecules* **1993**, *26*, 4055. (c) Yamamoto, T.; Maruyama, T.; Zhou, Z.; Ito, T.; Fukuda, T.; Yoneda, Y.; Begum, F.; Ikeda, T.; Sasaki, S.; Takezoe, H.; Fukada, A.; Kubota, K. *J. Am. Chem. Soc.* **1994**, *116*, 4832. (e) Zhu, S. S.; Swager, T. M. *Adv. Mater.* **1996**, *8*, 497. (f) Wang, B.; Wasielewski, M. R. *J. Am. Chem. Soc.* **1997**, *119*, 12.

(6) (a) Elliott, C. M.; Baldy, C. J.; Nuwaysir, L. M.; Wilkins, C. L. *Inorg. Chem.* **1990**, *29*, 389. (b) Pitt, C. G.; Bao, Y.; Seltzman, H. H. *J. Polym. Sci. Polym. Lett. Ed.* **1986**, *24*, 13. (c) Denisevich, P.; Abruna, H. D.; Leidner, C. R.; Meyer, T. J.; Murray, R. W. *Inorg. Chem.* **1982**, *21*, 2153.

(7) Hanabusa, K.; Higashi, J.; Koyama, T.; Shirai, H. *Makromol. Chem.* **1989**, *190*, 1.

(8) Kimura, M.; Horai, T.; Hanabusa, K.; Shirai, H. *Adv. Mater.* **1998**, *10*, 459.

(9) (a) Gould, S.; Strouse, G. F.; Meyer, T. J.; Sullivan, B. P. *Inorg. Chem.* **1991**, *30*, 2942. (b) Eaves, J. G.; Munro, H. S.; Parker, D. *J. Chem. Soc., Chem. Commun.* **1985**, 684.

(10) Jiang, B.; Yang, S. W.; Bailey, S. L.; Hermans, L. G.; Niver, R. A.; Bolcar, M. A.; Jones, W. E., Jr. *Coord. Chem. Rev.* **1998**, *171*, 365.

(11) (a) Peng, Z.; Yu, L. *J. Am. Chem. Soc.* **1996**, *118*, 3777. (b) Lee, J.-K.; Yoo, D.; Rubner, M. F. *Chem. Mater.* **1997**, *9*, 1710. (c) Elliott, C. M.; Pichot, F.; Bloom, C. J.; Rider, L. S. *J. Am. Chem. Soc.* **1998**, *120*, 6781. (d) Wang, Q.; Wang, L.; Yu, L. *J. Am. Chem. Soc.* **1998**, *120*, 12860.

(12) (a) Ng, P. K.; Gong, X.; Wong, W. T.; Chan, W. K. *Macromol. Rapid. Commun.* **1997**, *18*, 1009. (b) Chan, W. K.; Ng, P. K.; Gong, X.; Hou S. *J. Mater. Chem.* **1999**, 2103. (c) Wong, C. T.; Chan, W. K. *Adv. Mater.* **1999**, *11*, 455.

(13) (a) Ng, W. Y.; Chan, W. K. *Adv. Mater.* **1997**, *9*, 716. (b) Ng, W. Y.; Gong, X.; Chan, W. K. *Chem. Mater.* **1999**, *11*, 1165. (c) Yu, S. C.; Hou, S.; Chan, W. K. *Macromolecules* **1999**, *32*, 5251.

(14) (a) Yu, S. C.; Chan, W. K. *Macromol. Rapid Commun.* **1997**, *18*, 213. (b) Yu, S. C.; Gong, X.; Chan, W. K. *Macromolecules* **1998**, *31*, 5639.

(15) Chan, W. K.; Gong, X.; Ng, W. Y. *Appl. Phys. Lett.* **1997**, *71*, 2919,.

(16) *The Materials Science and Engineering of Rigid-Rod Polymers*; Adams, W. W., Edy, R. K., McLemore, D. E., Eds.; Symposium Proceeding Vol 134; Materials Research Society: Pittsburgh, PA, 1989.

(17) Yamazaki, N.; Matsumoto, M.; Higashi, F. *J. Polym. Sci.* **1975**, *12*, 1373.

(18) Nondek, L.; Malek, J. *Makromol. Chem.* **1977**, *178*, 2211.

(19) Habib, O. M. O.; Malek, J. *Collect. Czech. Chem. Commun.* **1976**, *41*, 1158.

(20) Jahnig, F. *J. Chem. Phys* **1979**, *70*, 3279.

(21) Ohtsuki, T. *Physica.* **1983**, *121A*, 513.

(22) Watanabe, J.; Harkness, B. R.; Sone, M.; Ichimura, H. *Macromolecules* **1994**, *27*, 507.

(23) Watanabe, J.; Sekine, N.; Nematsu, T.; Sone, M. *Macromolecules* **1996**, *29*, 4816.

(24) Damman, S. B.; Mercx, F. P. M.; Kootwijk-Damman, C. M. *Polymer* **1993**, *34*, 1891.

(25) Laus, M.; Ferruti, P.; Caretti, D.; Angeloni, A. S.; Galli, G.; Chiellini, E. *Thermochim. Acta.* **1990**, *162*, 179.

(26) Nam, J.; Fukai, T.; Kyu, T. *Macromolecules* **1991**, *24*, 6250.

(27) Lee, C. C.; Chu, S.-G.; Berry, G. C. *J. Polym. Sci., Polym. Phys Ed.* **1983**, *21*, 1573.

(28) Gailberger, M.; Bassler, H. *Phys. Rev. B* **1991**, *44*, 8643.

(29) Pfister, G. *Phys. Rev. B* **1977**, *16*, 3676.

(30) (a) Blatchford, J. W.; Jessen, S. W.; Lin, L.-B.; Gustafson, T. L.; Fu, D.-K.; Wang, H.-L.; Swager, T. M.; MacDiarmid, A. G.; Epstein, A. J. *Phys. Rev. B* **1996**, *54*, 9180. (b) Jessen, S. W.; Blatchford, J. W.; Lin, L.-B.; Gustafson, T. L.; Partee, J.; Shinar, J.; Fu, D.-K.; Marsella, M. J.; Swager, T. M.; MacDiarmid, A. G.; Epstein, A. J. *Synth. Met.* **1997**, *84*, 501.

(31) Doornbos, T.; Stratiing, J. *Org. Prep. Proc.* **1969**, *1*, 287.
(32) Bos, K. D.; Kraaijkamp, J. G.; Noltes, J. G. *Synth. Commun.* **1979**, *9*, 497.
(33) Evams, J. R.; Orwell, R. A.; Tang, S. S *J. Polym. Sci., Polym. Chem. Ed.* **1985**, *23*, 971.
(34) Sullivan, B. P.; Salmon, D. J.; Meyer, T. J. *Inorg. Chem.* **1978**, *17*, 3334.
(35) Sprintschnik, G.; Sprintschnik, H. W.; Kirsch, P. P.; Whitten, D. G. *J. Am. Chem. Soc.* **1977**, *99*, 4947.
(36) Muller-Horsche, E.; Haarer, D.; Scher, H. *Phys. Rev. B* **1987**, *35*, 1273.

MA991863J